CD13 is a novel mediator of monocytic/endothelial cell adhesion

Paola Mina-Osorio,* Beata Winnicka,* Catherine O'Conor,* Christina L. Grant,* Lotte K. Vogel,[†]
Daniel Rodriguez-Pinto,* Kathryn V. Holmes,[‡] Enrique Ortega,[§] and Linda H. Shapiro*,[1]

*Center for Vascular Biology, Department of Cell Biology, University of Connecticut Health Center, Farmington, Connecticut, USA; [†]Department of Medical Biochemistry and Genetics, The Panum Institute, University of Copenhagen. Denmark; [‡]Molecular Biology Program, University of Colorado at Denver and Health Sciences Center, Aurora, Colorado, USA; and [§]Department of Immunology, Instituto de Investigaciones Biomédicas, Universidad Nacional Autónoma de México, México

Abstract: During inflammation, cell surface adhesion molecules guide the adhesion and migration of circulating leukocytes across the endothelial cells lining the blood vessels to access the site of injury. The transmembrane molecule CD13 is expressed on monocytes and endothelial cells and has been shown to mediate homotypic cell adhesion, which may imply a role for CD13 in inflammatory monocyte trafficking. Here, we show that ligation and clustering of CD13 by mAb or viral ligands potently induce myeloid cell/endothelial adhesion in a signal transduction-dependent manner involving monocytic cytoskeletal rearrangement and filopodia formation. Treatment with soluble recombinant (r)CD13 blocks this CD13-dependent adhesion, and CD13 molecules from monocytic and endothelial cells are present in the same immunocomplex, suggesting a direct participation of CD13 in the adhesive interaction. This concept is strengthened by the fact that activated monocytic cells adhere to immobilized recombinant CD13. Furthermore, treatment with anti-CD13 antibodies in a murine model of peritonitis results in a decrease in leukocyte infiltration into the peritoneum, suggesting a potential role for CD13 in leukocyte trafficking in vivo. Therefore, this work supports a new direction for CD13 biology, where these cell surface molecules act as true molecular interfaces that induce and participate in critical inflammatory cell interactions. *J. Leukoc. Biol.* 84: 448–459; 2008.

INTRODUCTION

In response to injury or infection, the body mobilizes the cells of the immune system to initiate an inflammatory response at the site of damage. A critical step in this response is the adhesion of circulating leukocytes to the endothelial cells lining the blood vessels, allowing their subsequent migration across the endothelial cell barrier to access the insult. Damaged or infected tissues are rich in vasoactive peptides, chemoattractants, and other products that stimulate the endothelial cells and leukocytes to induce or activate cell surface molecules that mediate the adhesion and transmigration processes [1, 2].

Membrane-bound ectoenzymes have emerged recently as a group of surface molecules that participate in leukocyte activation and trafficking (reviewed in ref. [3]). Although proteolysis of vasoactive peptides and chemokines by ectoenzymes mediates leukocyte migration in some cases, frequently, they function independently of their enzymatic activity [4] by triggering signaling cascades that lead to calcium fluxes, cytoskeletal rearrangement, release of inflammatory mediators, and integrin activation or functionally or physically associating with adhesion molecules to regulate their signaling or shedding [3, 5].

CD13/aminopeptidase N (CD13) is an ectoenzyme that is predominantly expressed in monocytic cells and epithelial cells of the liver, intestine, and kidney [6] and more recently, has been shown to be potently up-regulated on the activated endothelial cells of angiogenic vasculature [7–9]. In addition to its enzymatic regulation of neuroregulatory and vasoactive peptides [10, 11], CD13 is the receptor for a prominent subgroup of coronaviruses including the human coronavirus 229E (HCoV-229E) [12]. Structurally, CD13 consists of a large extracellular domain containing the enzymatic active site, a transmembrane domain, and a short cytoplasmic tail with no known signaling motifs. Thus, it is believed that CD13 is intrinsically incapable of signaling and may function as a signal regulator of other molecules [13, 14]. Recently, we and others have reported that cross-linking CD13 by antibodies results in monocytic cell activation via signal transduction-dependent mechanisms [15, 17]. This activation is characterized by increased FcR-mediated phagocytosis [15], Ca^{++} flux, and cytokine secretion [16] and an increase in the adhesive

capacity of the cells [17]. The CD13-induced cell–cell adhesion was demonstrated to be dependent on the carbohydrate-binding protein galectin-3 and independent of CD13 enzymatic activity [18].

As CD13 regulates monocytic cell adhesion and is expressed on monocytes and endothelial cells, in the present work, we asked if CD13-mediated activation of monocytes and monocytic cells affects their capacity to adhere to and transmigrate through resting or activated endothelium in vitro and in vivo. Our results indicate that monocytic cell activation by ligand-mimicking antibodies or a natural CD13 ligand, HCoV-229E, results in a dramatic, signal transduction-dependent increase in adhesion to the endothelium that is distinct from that induced by inflammatory cytokines. This adhesion requires CD13 clustering and involves complexes containing monocytic and endothelial CD13, suggesting a direct participation of CD13 in this process. Importantly, blocking CD13 interactions with specific antibodies or soluble CD13 (sCD13) abrogates the effect. Finally, blocking CD13 interactions in vivo with specific antibodies results in a reduction in peritoneal leukocyte infiltration in a murine model of peritonitis, supporting a fundamental role for CD13 in leukocyte transendothelial migration into inflammatory sites.

MATERIALS AND METHODS

Cells and antibodies

Primary HUVEC (Cambrex Bioscience, Hopkinton, MA, USA) were maintained according to the provider's instructions. U-937 cells, WEHI-274.1 (murine myeloid cell line), C33A cells, and hemangioendothelioma (EOMA) cells [19] were from the American Type Cell Culture Collection (ATCC; Manassas, VA, USA). PBMC were from AllCells (Emeryville, CA, USA). Anti-CD13 mAb 452 and its $F(ab)'_2$ and Fab fragments were purified from the hybridoma donated by Dr. Meenhard Herlyn (The Wistar Institute, Philadelphia, PA, USA). mAb anti-CD13 WM-4.7 and WM-15 were from Sigma Chemical Co. (St. Louis, MO, USA) and BD PharMingen (San Diego, CA, USA), respectively. Anti-CD13 mAb Y2-K has been described previously [20]. Hamster anti-mouse CD13 mAb K1 was purified from the hybridoma provided by Dr. William Paul {National Institutes of Health (NIH), Bethesda, MD, USA [21]}. Hamster IgG was from BioLegend (San Diego, Ca, USA). Anti-CD18 mAb IB4 was a gift of Dr. William Muller (Cornell University, Ithaca, NY, USA). mAb anti-P-selectin G1/G1-4 and anti-E-selectin HAE-1f were from Ancell Corp. (Bayport, MN, USA). mAb anti-CD54 RR1/1 was from Alexis Biochemicals (Switzerland). mAb anti-CD31 hec7 was from Pierce Biotechnology (Rockford, IL, USA). Mouse IgG1 control and goat anti-mouse (GAM) $F(ab)'_2$ fragments were from Sigma Chemical Co. FITC-labeled GAM $F(ab)'_2$ fragments were from Beckman Coulter (Fullerton, CA, USA).

Expression of recombinant (r)DNA constructs

Amplified, full-length human CD13 (hCD13) cDNA [6] was purified and subcloned into the XhoI/SacII site of the pEGFP-C1 vector (BD Clontech, Mountain View, CA, USA) by PCR cloning. C33A and EOMA cells were stably transfected using Lipofectamin 2000 (Invitrogen, Carlsbad, CA, USA), according to the manufacturer's instructions. Selection was carried out using Geneticin (Gibco, Grand Island, NY, USA) at a concentration of 600 μg/ml. Cells were sorted using a FACSVantage flow cytometer (BD PharMingen).

Quantitative adhesion assays

HUVEC (0.5×10^6/ml) were seeded on fibronectin-coated (10 μg/ml), 96-well plates and grown to confluency for 24–48 h in EBM-2 medium (Cambrex, East Rutherford, NJ, USA). Subsequently, untreated or anti-CD13 mAb-treated (1 μg/ml), calcein-labeled monocytic cells were added to the monolayers, and adhesion was allowed to proceed for 15 min or as indicated. Each condition was assayed in triplicate. Unbound monocytic cells were washed away, and the remaining cells were lysed. For a detailed description, see Supplemental Methods. Fluorescence was quantified in a CytoFluor 4000 (PerSeptive Biosystems, Framingham, MA, USA). Data represent the fluorescence obtained from each sample normalized against the fluorescence corresponding to cells adhered onto untreated controls. The same protocol was used for adhesion assays with C33A transfectant cells. For blocking experiments with recombinant sCD13, mAb-treated monolayers or monocytic cells were washed three times and subsequently incubated with the indicated concentration of sCD13 for 30 min at 37°C. The unbound protein was washed away, and adhesion was allowed to proceed in the presence of more protein at the same concentration or its vehicle (PBS) in equivalent volumes as indicated. HCoV-229E was obtained from the ATCC (VR-740) and propagated in the human MRC-5 lung cell line at 34°C, also obtained from ATCC. The virus was titered by plaque assay in MRC-5 cells at 34°C. The virus from supernatant was purified by ultracentrifugation as described previously for murine coronavirus murine hepatitis virus [22]. Briefly, virions at the interface between 30% sucrose and 50% sucrose in Tris maleate saline buffer (TMS; pH 6.5) were harvested and further purified by equilibrium ultracentrifugation in a 20–50% sucrose density gradient in TMS. The virus band was dialyzed to remove the sucrose, suspended in DMEM, high glucose, with 10% FBS and 2% penicillin, streptomycin, and fungizone (Gibco). The virus was UV-irradiated, and residual infectivity was determined by plaque assay. The titers of virus before and after irradiation were 4.5×10^6 PFU/ml and <1 PFU/ml, respectively. Aliquots of the UV-irradiated virus were stored at −80°C. Adhesion experiments were carried out as above using concentrations of the virus that correspond to the multiplicities of inoculation indicated prior to UV irradiation.

sCD13 adhesion assays

Wells of a 96-well plate (Reacti-bind™, Pierce Biotechnology) were coated with sCD13 at the indicated concentrations in PBS overnight at 4°C. After three washes, they were blocked with PBS/1% BSA for 2 h at room temperature. Calcein-labeled U-937 cells were pretreated with 0.5 μg/ml of the anti-CD13 mAb 452 for 30 min at 37°C, washed three times, and added to the sCD13-coated plate for 30 min at 37°C. Plates were washed seven times with PBS, and adhesion was quantified by fluorometry as described above.

Immunoprecipitation and immunoblot

C33A cells [nontransfected and stably expressing the empty vector, the truncated form of CD13 (tCD13), or full-length hCD13] were grown to confluency on 100 mm culture dishes. U-937 cells (1.2×10^7) were preincubated with a biotinylated anti-CD13 mAb 452 (2 μg/ml) for 30 min at 37°C. After several washes, the cells were allowed to adhere for 20 min. The monolayers and adherent monocytic cells were scraped in the presence of lysis buffer (Tris 10 mM, NaCl 150 mM, glycerol 5%, Triton X-100 1%) containing EDTA-free protease inhibitor (Roche, Nutley, NJ, USA). Nonadherent U-937 cells were collected separately, pelleted, lysed, and mixed with the adherent lysates to obtain the same amount of protein from monocytic cells in all samples. Monocytic cell CD13 was precipitated with streptavidin-agarose beads (Invitrogen) for 2 h at 4°C. Immunoprecipitated proteins were separated on 10% SDS-PAGE and transferred onto polyvinylidene difluoride membranes (Millipore, Bedford, MA, USA). CD13 from C33A cells was detected with an anti-V5 mAb (1:3000 dilution, Invitrogen), followed by a HRP-conjugated antibody (Amersham Biosciences, Piscataway, NJ, USA). Chemiluminescent signals were detected using Immobilon™ chemiluminescent HRP substrate (Millipore). After stripping with 0.1 M glycine (pH 2.5) and blocking, the same membranes were blotted using HRP-conjugated streptavidin (Pierce Biotechnology).

Murine peritonitis

Five-week-old FVB female mice (Charles River Laboratories, Portage, MI, USA) were anesthetized with an i.p. injection of Avertin (prepared using 2.5 g 2,2,2-tribromoethanol, 5 ml 2-methyl-2-butanol, and 200 ml distilled water). Peritonitis was induced by an i.p injection of thioglycollate (3 ml) [23]. Subsequently, a 3-mg/kg dose of a hamster anti-mouse, anti-CD13 mAb (clone K1) in sterile saline was injected i.v. into the retro-orbital space. As controls, the same volume of saline or azide-free hamster IgG, which was adjusted to an

equivalent volume, was injected into control animals. Peritoneal cells were collected 16 h later and counted using a Neubauer hemocytometer. Subsequently, the cells were fixed on slides with 2% paraformaldehyde and stained with H&E for differential determination of the number of mononuclear versus polymorphonuclear cells. At this time-point, a significant increase in the number of recruited macrophages has been reported [23, 24]. Immediately after euthanasia, a 100-μl sample of peripheral blood was collected by cardiac puncture. Erythrocytes were lysed by hypotonic shock, and the remaining leukocytes were fixed, stained with Gr1 and CD11b antibodies, and analyzed by flow cytometry. Paraffin sections of peritoneal tissues were stained with H&E and photographed using a Zeiss Axiovert microscope with a 20× objective. All animal procedures were approved by the University of Connecticut Health Center Animal Care Committee (Farmington, CT, USA).

RESULTS

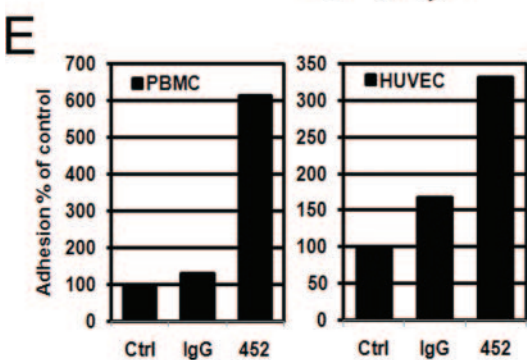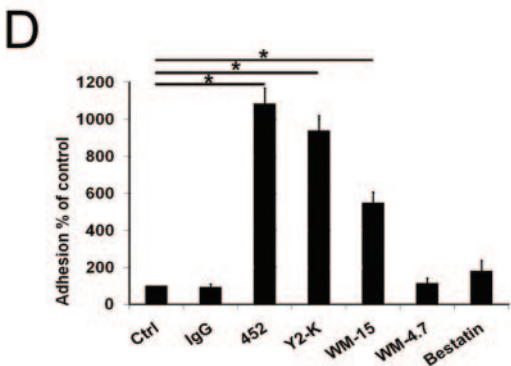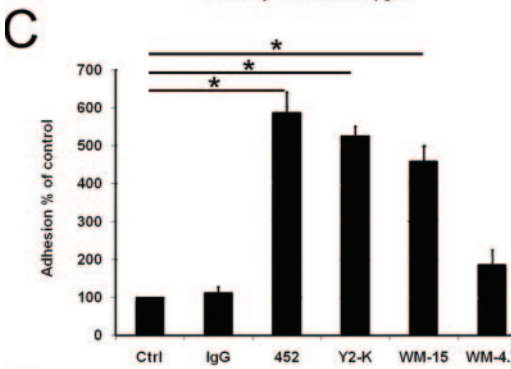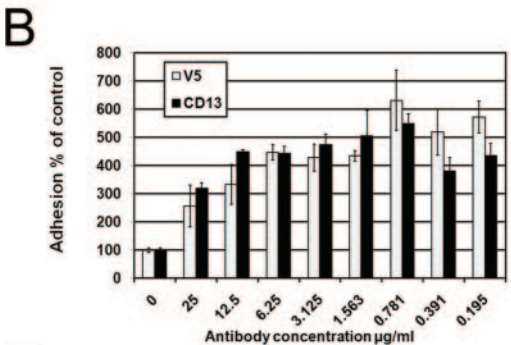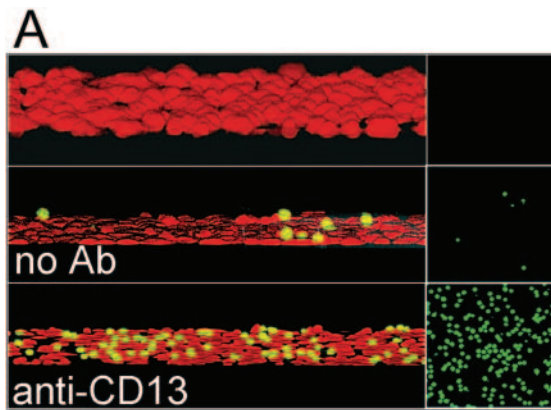### CD13 engagement induces monocytic cell/endothelial adhesion

In previous studies, we observed that pretreatment of monocytes and monocytic cells with anti-CD13 mAb induced rapid cell–cell adhesion in a signal transduction-dependent but enzymatic activity-independent manner [17]. As CD13 is expressed on monocytes and the endothelial cells of tumor vessels [7, 9], vessels in the ischemic heart [25], and has been shown to be up-regulated by inflammatory cytokines [26–29], we asked if ligation of CD13 would influence the monocyte/endothelial interactions that are critical to monocyte trafficking during inflammation. Pretreatment of primary HUVEC (which express high levels of CD13 in response to growth factors in the culture medium [8, 9]) with the anti-CD13 mAb 452 prior to addition of labeled U-937 monocytic cells significantly induced monocytic cell adhesion (**Fig. 1A**). Importantly, adhesion was not induced when cells were pretreated with mAb at 4°C (data not shown), suggesting that the induction of adhesion was an active process and that it was not a result of cell–cell association via unbound Fab portions of the mAb binding to CD13 molecules on the opposite cell. To strengthen this conclusion, we produced stable cell lines expressing the V5 epitope-tagged, full-length hCD13 in a CD13-negative human epithelial cell line C33A (hCD13-C33A) and assayed these for antibody-induced monocytic cell adhesion. Although the high expression of CD13 on these transfectants had no effect on the basal adhesion of monocytic cells (see Fig. 3C), pretreatment of the hCD13-C33A with anti-CD13 mAb 452 or an anti-V5 antibody was capable of inducing similar increases in adhesion over a wide range of doses, although maximal induction was observed with low antibody concentrations (Fig. 1B). As the V5 epitope is only expressed by the cells in the monolayer, this result clearly demonstrates that anti-CD13-dependent adhesion is not the result of single antibodies simultaneously binding to the CD13 on both cell populations but more likely by influencing the intrinsic, adhesive properties of the cells.

We expanded our investigation using three additional anti-CD13 mAb of varying epitope specificities to pretreat HUVEC (summarized in **Table 1**). Maximal induction of monocytic cell-endothelial cell adhesion was observed with two independent mAb, 452 and Y2-K (Fig. 1C), which recognize a common epitope (Supplemental Fig. 1) that has been shown to be important for HCoV-229E infection [20]. In contrast, pretreat-

ment of HUVEC with the WM-15 mAb that recognizes a distinct epitope and inhibits CD13 enzymatic activity [31] showed a more modest, yet significant induction of monocytic cell adhesion. A third reagent, mAb WM-4.7, does not inhibit viral infection, does not block enzymatic activity [31, 32], and as expected, had no effect on monocytic cell adhesion to HUVEC, nor did treatment of cells with bestatin, a chemical inhibitor of CD13 enzymatic activity. Interestingly, pretreatment of the adhering monocytic cells with anti-CD13 mAb prior to addition of the untreated endothelial monolayer produced an identical pattern of antibody-dependent adhesion (Fig. 1D), with an even higher effect than when pretreating HUVEC (average 54.1% higher adhesion of treated U-937 vs. treated HUVEC). Thus, it would appear that shared critical regions of the CD13 molecule participate in each of its various functions and that CD13 ligation affects adhesion properties of monocytic cells and endothelial cells. Importantly, when primary PBMC were used in place of the U-937 cell line, we observed a similar dramatic increase in adhesion to HUVEC when the PBMC or HUVEC were pretreated with the mAb (Fig. 1E). Similarly, primary macrophages and lung microvascular endothelial cells behave analogously (see Supplemental Fig. 5). As monocytes and a small percentage of granulocytes are the only CD13$^+$ populations in PBMC, these results clearly demonstrate that ligation of endothelial or myeloid cell CD13 with specific antibodies induces adhesion of primary myeloid cells and monocytic cell lines. Thus, the U-937 cell line is a valid model for primary monocyte/endothelial interactions, as previously reported [34–37]. We determined the kinetics of CD13-induced adhesion to endothelial monolayers (Supplemental Fig. 2). Although pretreatment with anti-CD13 antibodies for various time periods rapidly induced significant adhesion, the adhesion appears to be transient, where the number of monocytic cells attached to the monolayer decreases progressively, perhaps suggesting that subsequent to initial adhesion, the cells become refractory and are no longer able to adhere.

The ability of anti-CD13 mAb to stimulate adhesion depends on their capacity to induce CD13 clustering

Many anti-receptor bodies mimic ligand binding by cross-linking their receptor targets and thus, trigger subsequent signal transduction. In experiments to determine if the differences in the ability of anti-CD13 antibodies to induce adhesion were a result of their ability to cross-link CD13 molecules on the cell surface, we found that F(ab)′$_2$ fragments of the 452 mAb but not its Fab fragments were capable of inducing monocytic cell adhesion when preincubated with U-937 cells (**Fig. 2A**), and the binding capacity of the two reagents was comparable (Fig. 2A, inset). Similarly, cross-linking of the nonactivating mAb WM-4.7 with F(ab)′$_2$ fragments of a secondary antibody results in high levels of adhesion similar to those obtained with equivalent fragments of the mAb 452. Identical results were obtained with HUVEC (not shown). In addition, as the antibody fragments are capable of inducing adhesion, this effect is not mediated by FcRs on the opposite cell. CD13 clustering by activating but not inactive antibodies can be visualized by confocal imaging of U-937 cells treated with fluorescently labeled antibodies, where only the adhesion-

inducing 452 mAb but not the noninducing WM-4.7 can cluster CD13 molecules on the cell surface (Fig. 2B). Similar CD13 aggregates were observed when HUVEC (Supplemental Fig. 3, A and B), hCD13-C33A cells (not shown), or a mouse endothelial cell line (EOMA, Fig. 2B) expressing GFP-tagged hCD13 were treated with the 452 mAb as compared with untreated cells. Thus, as reported for homotypic aggregation (HA) [17], clustering of membrane-bound CD13 is required to alter the adhesive properties of the cell.

Binding HCoV-229E to its receptor, CD13, results in CD13 cross-linking and subsequent infection [38]. Interestingly, we have shown that maximal induction of adhesion was obtained by cross-linking CD13 with an antibody that efficiently blocks the binding of HCoV-229E to CD13 (Y2-K, Fig. 1C), suggesting that ligand binding to this particular epitope may be a common initiator of CD13 cell adhesion and virus entry activities. To further delineate the scope of induction of adhesion by CD13 cross-linking and to determine if natural ligands that cross-link CD13 also induce monocytic cell/endothelial cell adhesion, we tested the effect of treatment of monocytic cells with UV-irradiated HCoV-229E. Monocytic cells treated with inactivated virus (which contain ~200 trimeric spikes/virion) showed a dose-dependent increase in adhesion (Fig. 2C). The dose/response curve suggests a cross-linking-dependent process. Taken together, these results demonstrate that clustering of CD13 by a specific mAb or by a natural multivalent ligand, HcoV-229E, increases cell adhesiveness. This process may be exploited by the virus to manipulate immune cell behavior.

CD13 expression in the monolayers is required for mAb-treated monocytic cells to adhere

In anti-CD13-induced monocytic aggregation, CD13 actively redistributes to the zones of cell–cell contact [17], and treatment with excess antibody abrogates cell–cell adhesion, raising the possibility that CD13 may actively participate in adhesion [18]. To investigate if CD13 localization on endothelial or other target cells would also support a role for CD13 as an

Fig. 1. CD13 ligation induces monocytic cell adhesion to endothelial mono-layers. (A) Three-dimensional (3-D) reconstructions of calcein red-labeled HUVEC monolayers untreated (middle) or treated with anti-CD13 mAb (1.0 μg/ml, bottom) after adhesion of calcein green-labeled U-937 cells. The top images show HUVEC monolayers without U-937 cells to demonstrate the absence of fluorescence bleed-through between channels. The right panels represent the green channel-only images at the plane of focus of the monocytic cells. Images representative of three independent experiments are shown. (B) C33A cells expressing V5-tagged CD13 were incubated with anti-CD13 (452; 1.0 μg/ml) or anti-V5 mAb at the doses indicated and washed, and monocytic cells were allowed to adhere for 15 min. Adhesion was quantified by fluorometry, as described in Materials and Methods. The graph is representative of the arithmetic mean and the SD of two independent experiments. (C) HUVEC monolayers were preincubated with the indicated anti-CD13 mAb (1.0 μg/ml), an isotype-matched IgG, or the CD13 inhibitor bestatin (100 μM). After washing, U-937 cells were allowed to adhere for 15 min. The percentage of adherent cells as compared with untreated cells [control (Ctrl)] is shown. The graph represents the arithmetic mean and SD of six independent experiments. (D) The same experiment as in C but preincubating U-937 cells with the indicated mAb. The graph represents the arithmetic mean and SD of five independent experiments. (E) PBMC (left) or HUVEC (right) were incubated with 452 mAb for 30 min and 1 h, respectively. Adhesion was quantified as above. *, $P < 0.05$, unpaired Student's t-test between the individual treatment condition and the control.

TABLE 1. Activities of CD13 Reagents

Reagent	Epitope recognized	Inhibits enzymatic activity	Inhibits virus binding	Clusters CD13	Induces adhesion	Reference
452 mAb	"A"	yes	ND	yes	yes	[30]
Y2-K mAb	"A"	yes	yes	yes	yes	[20]
WM-15 mAb	"B"	yes	no	yes	yes	[31]
WM-4.7 mAb	"C"	no	no	no	no	[31, 32]
Bestatin	Active site	yes	no	no	no	[33]

ND, Not determined.

adhesion molecule, we assessed the distribution of CD13 on GFP-tagged, CD13-expressing C33A or EOMA cells (**Fig. 3A**) or on HUVEC monolayers stained with immunofluorescently labeled anti-CD13 mAb (Supplemental Fig. 3C). In isolated cells of all types studied, CD13 was relatively evenly distributed in the cell membrane (Fig. 3A and Supplemental Video 1) but appeared to concentrate at points of contact when other cells were encountered, as previously reported in other cell types (ref. [30]; Figs. 3A, center, and 2B). Similarly, live-cell imaging of mAb-treated monocytic cells adhering to untreated C33A cells expressing a GFP-tagged CD13 showed that CD13 was strongly expressed in filopodial structures protruding from the monolayer toward the adhering monocytic cells (Fig. 3A, right, and Supplemental Videos 2–4). Analogous structures termed "microvilli-like projections" [39] or "endothelial docking structures" [40] have been observed during leukocyte adhesion and transmigration, further supporting a role for CD13 in these processes.

Strengthening this notion, concurrent treatment of the monocytic cell and endothelial cell populations with anti-CD13 mAb or alternatively, adhesion in the continued presence of anti-CD13 mAb resulted in an extremely modest increase in adhesion when compared with treatment of individual cell populations (Fig. 3B, and data not shown), suggesting blockade of a homophilic interaction between monocytic and endothelial CD13 molecules that might be participating directly in the adhesion process. If this were the case, CD13 must be expressed on both cell types for antibody-induced adhesion to occur. Indeed, as shown in Figure 3C, using the V5-tagged, CD13-transfected cells described above (hCD13-C33A), we found that anti-CD13, mAb-activated monocytic cells bind exclusively to CD13-expressing monolayers and not to nontransfected or vector-transfected controls, demonstrating that its expression is required to mediate adhesion. Additionally, mAb-treated monocytic cells did not bind to mAb-blocked hCD13-C33A monolayers, presumably by blocking CD13 homophilic interactions. Therefore, CD13 accumulates in endothelial docking structures and is required on the monolayers for binding of anti-CD13-activated monocytic cells.

Monocytic CD13 is present in a complex with endothelial CD13

Although the previous experiments imply a CD13–CD13 interaction, they do not directly address if the monocytic CD13 is associated with CD13 expressed on the monolayer. To investigate this question, U-937 cells were activated with a biotinylated form of anti-CD13 mAb 452, washed, and allowed to adhere to V5-tagged, CD13-transfected monolayers (hCD13-C33A). Monocytic CD13 was immunoprecipitated from total lysates of these cocultures using streptavidin beads, and the resulting complexes were probed for the presence of the monolayer-expressed V5 epitope (**Fig. 4A**). V5-tagged proteins corresponding to the molecular weight of mature CD13 were readily apparent in lysates from conditions containing monolayers expressing full-length CD13 but not on nontransfected or vector-transfected control monolayers or cells expressing a V5-tagged tCD13 lacking the extracellular domains (htCD13), verifying the specificity of the precipitated band. Importantly, a nonspecific interaction with the V5 epitope is ruled out by the lack of V5-tagged tCD13 in complexes with immunoprecipitated monocytic cell CD13 (not shown). Similarly, excess antibody is not responsible for the coimmunoprecipitation, as V5-tagged proteins are not precipitated when the individual populations are first lysed and then mixed prior to immunoprecipitation, thus preventing endothelial/monocytic cell interaction (data not shown). Additionally, we observed a dose-dependent abrogation of adhesion of mAb-activated monocytic cells to HUVEC when the monocytic cells were treated with a truncated recombinant sCD13 [20], even when the protein was no longer present during the adhesion assay, and basal adhesion was unaffected, further supporting a direct CD13–CD13 interaction (Fig. 4B). However, in the reciprocal experiment, treatment of mAb-activated HUVEC with sCD13 showed a significant but clearly less efficient inhibition of adhesion (Fig. 4C), unless the protein was allowed to remain during the assay, signifying that it preferentially binds to mAb-treated, monocytic cells as compared with mAb-treated HUVEC. This suggests a more complex CD13–CD13 interaction that may involve the exposure of auxiliary molecules or ligands on monocytic cells after CD13 clustering and that the soluble form of the protein is capable of regulating this interaction. Alternatively, differential glycosylation of the CD13 molecule may play a role, as it has been proposed that at least five different glycoforms of CD13 exist [32, 41]. Finally, mAb-treated but not resting monocytic cells specifically adhered to immobilized, purified sCD13 in a dose-dependent manner (Fig. 4D), confirming that CD13 can function as an adhesion molecule to mediate the interaction of monocytic cells with target cells.

CD13-induced monocytic cell–endothelial cell adhesion is signal transduction-dependent and involves actin polymerization

As it appears that expression of CD13 on target cells is sufficient to bind anti-CD13, mAb-activated monocytic cells, it
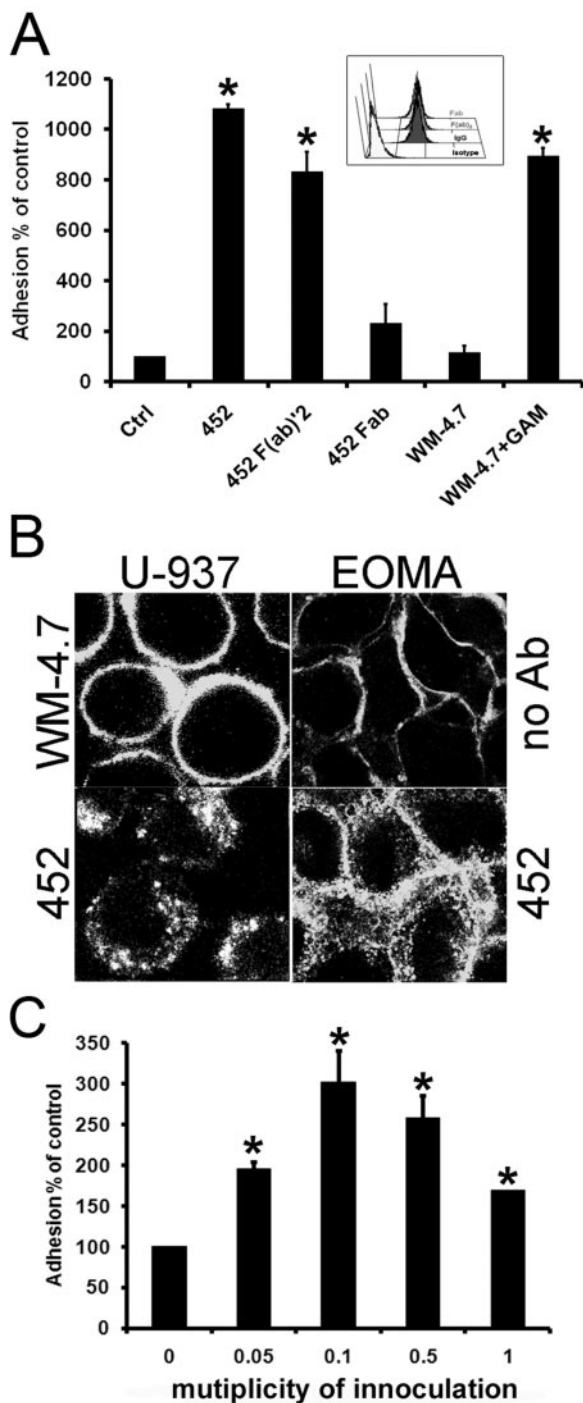
Fig. 2. The effect of anti-CD13 mAb in adhesion depends on CD13 cross-linking. (A) U-937 cells were incubated for 30 min with anti-CD13 mAb 452, its F(ab)′$_2$ or Fab fragments, or with the anti-CD13 mAb WM-4.7 alone or followed by a 30-min incubation with F(ab)′$_2$ fragments of a GAM antibody, all at 1.0 μg/ml. Fragments of the 452 mAb showed similar binding capacity as the complete mAb (IgG), as determined by FACS (inset). (B) Confocal imaging of U-937 cells treated with FITC-conjugated, anti-CD13 mAb WM-4.7 (1.0 μg/ml, upper left) or Texas-Red™-conjugated mAb 452 (1.0 μg/ml, lower left) for 15 min at 37°C. EOMA cells stably expressing hCD13-GFP were imaged before (upper right) or after (lower right) treatment with the mAb 452 (1.0 μg/ml) for 15 min at 37°C. (C) U-937 cells were incubated with UV-inactivated HCoV-229E for 1 h at 37°C at doses corresponding to the indicated multiplicity of innoculation. Unbound virus was washed away, and cells were allowed to adhere to HUVEC for 20 min at 37°C. Arithmetic mean and SD of three independent experiments are shown. *, $P < 0.05$, unpaired Student's t-test between the individual treatment condition and the control, untreated condition in each panel.

is possible that these CD13 homophilic interactions are the result of a passive association between the extracellular CD13 on the target monolayers and CD13 or its ligand on monocytic cells after clustering. However, antibody-induced adhesion requires signal transduction cascades in monocytic cells and endothelial cells, as preincubation of either cell type with the tyrosine kinase inhibitor herbimycin prior to antibody treatment profoundly inhibited antibody-induced adhesion with no effect on basal adhesion at the concentrations used (**Fig. 5A**). In contrast, G protein-coupled receptor signaling is not involved, as pretreatment of the monocytic cells with pertussis toxin prior to antibody activation did not affect CD13-induced adhesion (data not shown). These results suggest that the adhesion induced by CD13 ligation requires signaling cascades in both cell types and that blocking these mechanisms in one cell population influences the induction of adhesion by CD13 ligation on the opposite cell. Interestingly, the signaling cascades triggered in monocytic cells consistently appear to predominate over those induced in HUVEC, as adhesion is always more potently affected when monocytic signal transduction mechanisms are inhibited, regardless of which cell type is treated with the mAb (Fig. 5A).

An important consequence of tyrosine kinase signal transduction is actin polymerization, which is absolutely required for monocyte adhesion to target cells [42, 43]. We have shown that during anti-CD13 mAb-induced monocytic adhesion, CD13 is clearly concentrated at the leading edge of monocytic cells that are migrating toward cellular aggregates and is actively redistributed to the zones of cell–cell contact in aggregated cells [17]. Similarly, CD13 redistributes to the phagocytic cups during FcγR-mediated phagocytosis [15] and is enriched at the leading edge and in the membrane projections of endothelial cells (Fig. 3A), demonstrating that CD13 frequently accumulates at the sites of actin microfilament-driven processes. To determine whether microfilament assembly plays a role in CD13-induced adhesion, we inhibited this process with cytochalasin-D and assessed adhesion following anti-CD13 mAb treatment of endothelial cells (Fig. 5B) or monocytic cells (Fig. 5C). When endothelial cell CD13 is ligated, CD13-induced adhesion is essentially unaffected by blocking endothelial actin polymerization (Fig. 5B, Lanes 2 and 3). This is analogous to previous reports studying microvillar structures during leukocyte trafficking (similar to those in Fig. 3A) in TNF-α-activated endothelial cells [39, 44]. In contrast, pretreatment or persistent treatment of monocytic cells with cytochalasin-D completely abrogated adhesion to CD13-activated endothelial cells regardless of the status of endothelial cell actin polymerization (Fig. 5B, Lanes 4 and 5), again implying that the downstream consequences of ligation of monocytic CD13 have a greater impact on adhesion than those in endothelial cells. Similarly, in the reciprocal experiment (Fig. 5C), CD13-activated monocytic cells preincubated with cytochalasin-D showed a nearly 70% decrease in adhesion (Fig. 5C, Lane 3) and complete abrogation when the inhibitor was present during the entire assay (not shown) or when both cells are pretreated (Fig. 5C, Lane 5). In addition, cytochalasin treatment of HUVEC did not affect adhesion of mAb-treated monocytic cells (Fig. 5C, Lane 4), clearly demonstrating that microfilament assembly is a principal consequence of CD13-
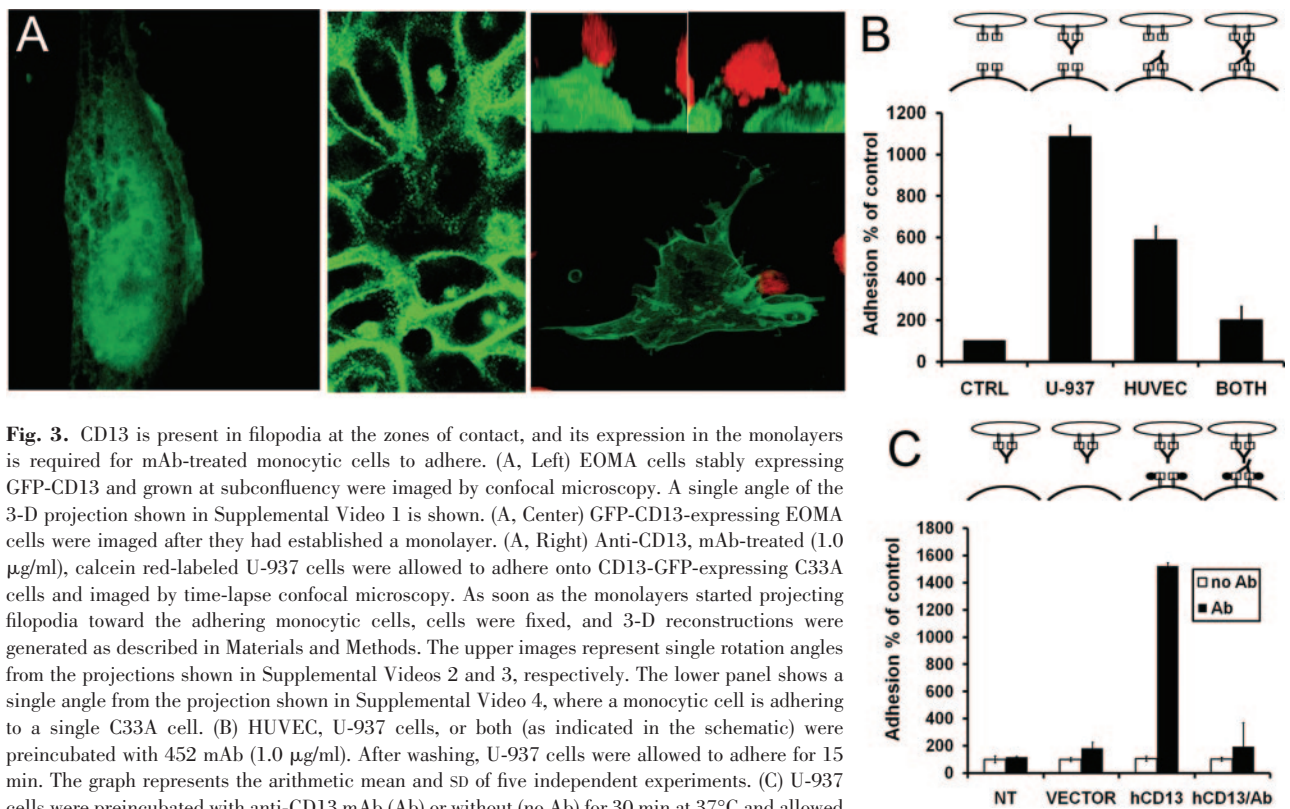
Fig. 3. CD13 is present in filopodia at the zones of contact, and its expression in the monolayers is required for mAb-treated monocytic cells to adhere. (A, Left) EOMA cells stably expressing GFP-CD13 and grown at subconfluency were imaged by confocal microscopy. A single angle of the 3-D projection shown in Supplemental Video 1 is shown. (A, Center) GFP-CD13-expressing EOMA cells were imaged after they had established a monolayer. (A, Right) Anti-CD13, mAb-treated (1.0 μg/ml), calcein red-labeled U-937 cells were allowed to adhere onto CD13-GFP-expressing C33A cells and imaged by time-lapse confocal microscopy. As soon as the monolayers started projecting filopodia toward the adhering monocytic cells, cells were fixed, and 3-D reconstructions were generated as described in Materials and Methods. The upper images represent single rotation angles from the projections shown in Supplemental Videos 2 and 3, respectively. The lower panel shows a single angle from the projection shown in Supplemental Video 4, where a monocytic cell is adhering to a single C33A cell. (B) HUVEC, U-937 cells, or both (as indicated in the schematic) were preincubated with 452 mAb (1.0 μg/ml). After washing, U-937 cells were allowed to adhere for 15 min. The graph represents the arithmetic mean and SD of five independent experiments. (C) U-937 cells were preincubated with anti-CD13 mAb (Ab) or without (no Ab) for 30 min at 37°C and allowed to adhere onto monolayers of nontransfected (NT), vector-transfected (VECTOR), or V5-tagged, hCD13-transfected C33A cells in the absence (hCD13) or presence (hCD13/Ab) of excess anti-CD13 mAb. Each bar represents the arithmetic mean and SD of three independent experiments.

induced signal transduction in monocytic cells. Accordingly, visualization of actin dynamics in CD13-activated monocytic cells with fluorescently labeled phalloidin showed that CD13 cross-linking induced the striking formation of numerous actin-rich, filopodia-like protrusions after antibody activation when compared with untreated cells (Fig. 5D) at time periods consistent with kinetics of antibody-induced adhesion. Similar to this observation, treatment of monocytic cells with activating antibodies induces Ca fluxes (Supplemental Fig. 4 and refs. [16, 45]). In contrast, antibody-treated HUVEC showed no discernable difference in actin localization (data not shown) in agreement with the cytochalasin inhibition data and arguing that CD13 cross-linking in endothelial cells induces downstream consequences that are qualitatively distinct from those seen in monocytic cells.

Ligation of CD13 impairs transendothelial migration in vivo

Increased adhesion of circulating leukocytes to endothelial cells would be predicted to enhance the ability of the cells to migrate across the endothelial cell monolayer to the sites of inflammation [1, 46, 47]. To determine the effects of CD13 ligation on inflammatory transendothelial migration in vivo, we induced peritonitis in mice treated i.v. with either vehicle, control IgG, or anti-murine CD13 antibodies (which we determined can induce monocytic cell adhesion; Supplemental Fig. 5), and assessed leukocyte infiltration into the peritoneal cavity. Surprisingly, although both cohorts of control animals showed an intense leukocyte infiltration into the peritoneal wall

that correlated with the number of peritoneal leukocytes, these numbers were clearly reduced in the anti-CD13 mAb-treated animals (**Fig. 6, A–C**). Interestingly, at this early time-point (16 h), the relative representation of infiltrating granulocytes versus mononuclear cells in the peritoneal fluid did not appear to be affected by anti-CD13 mAb treatment, as determined by direct quantification of the relative number of harvested peritoneal cells (Fig. 6D). Additionally, direct assessment of peripheral blood cell populations by FACS analysis of monocytes (CD11b+/Gr1−) and neutrophils (CD11b/Gr1 double-positive, Fig. 6E) showed equivalent numbers in anti-CD13-treated animals when compared with controls, arguing against antibody-induced cell death as a mechanism for reduced peritoneal infiltration. Therefore, our results indicate that ligation of CD13 significantly affects leukocyte trafficking in vivo and suggest it contributes to inflammatory processes through complex mechanisms.

DISCUSSION

We have previously reported that treatment of human monocytic cells with anti-CD13 mAb potently induces HA in a signal transduction-dependent manner [17]. Here, we demonstrate that ligation of CD13 on primary human myeloid cells or monocytic cell lines also promotes their adhesion to endothelial cells under in vitro static conditions, which importantly, we find is recapitulated in preliminary studies in physiologic flow (data not shown). We show that the induction of adhesion is
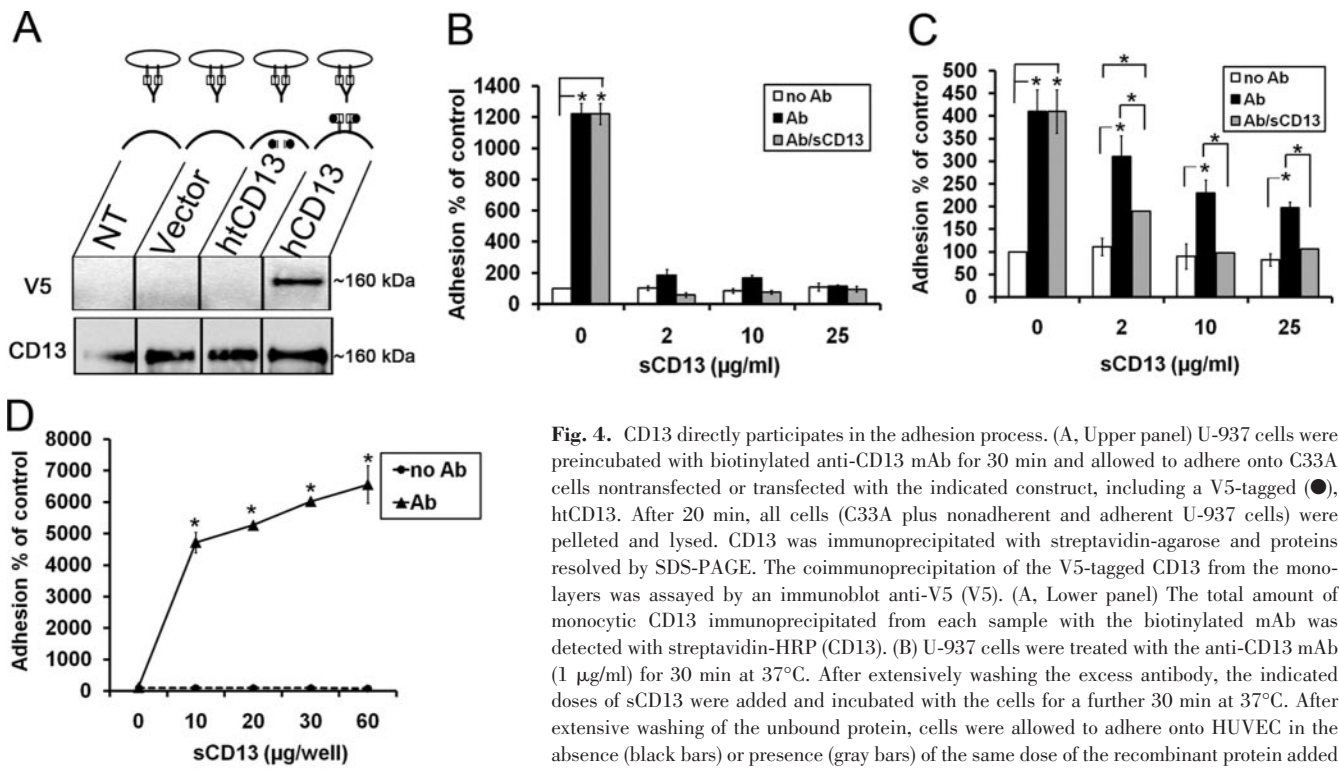
Fig. 4. CD13 directly participates in the adhesion process. (A, Upper panel) U-937 cells were preincubated with biotinylated anti-CD13 mAb for 30 min and allowed to adhere onto C33A cells nontransfected or transfected with the indicated construct, including a V5-tagged (●), htCD13. After 20 min, all cells (C33A plus nonadherent and adherent U-937 cells) were pelleted and lysed. CD13 was immunoprecipitated with streptavidin-agarose and proteins resolved by SDS-PAGE. The coimmunoprecipitation of the V5-tagged CD13 from the monolayers was assayed by an immunoblot anti-V5 (V5). (A, Lower panel) The total amount of monocytic CD13 immunoprecipitated from each sample with the biotinylated mAb was detected with streptavidin-HRP (CD13). (B) U-937 cells were treated with the anti-CD13 mAb (1 µg/ml) for 30 min at 37°C. After extensively washing the excess antibody, the indicated doses of sCD13 were added and incubated with the cells for a further 30 min at 37°C. After extensive washing of the unbound protein, cells were allowed to adhere onto HUVEC in the absence (black bars) or presence (gray bars) of the same dose of the recombinant protein added immediately before the assay. The graph represents the arithmetic mean and SD of two independent experiments. (C) The same experiment as in B was conducted but preincubating HUVEC with anti-CD13 mAb. After extensive washing, sCD13 was added and incubated for 30 min at 37°C. The protein was washed away, and monocytic cells were allowed to adhere in the absence (black bars) or presence (gray bars) of the same dose of protein added before the assay. (D) Untreated (no Ab) or anti-CD13 mAb-treated U-937 cells (Ab) were allowed to adhere onto the wells of a plate coated with the indicated amounts of sCD13 as described in Materials and Methods. The graph represents the arithmetic mean and SD of two independent experiments normalized against the control of BSA-coated wells as determined by fluorometry. *, $P < 0.05$, unpaired Student's T-test between indicated conditions (B, C) or untreated control (D).

strictly dependent on the ability of antibodies to cluster CD13 and requires active tyrosine kinases and CD13 expression on monocytic cells and endothelial cells. Accordingly, the multivalent CD13L, HCoV-229E (which specifically binds and clusters CD13), also induced monocytic cell adhesion to endothelial cells. Thus, treatment of monocytic cells with clustering antibodies functionally duplicates the response to CD13 cross-linking via a natural ligand, underscoring the potential in vivo relevance of this process and demonstrating the use of these antibodies as ligand-mimicking reagents to study CD13-mediated receptor functions.

In this study, we demonstrate that immunocomplexes from interacting cells contain monocytic and endothelial CD13 and that like most adhesion molecules [48–50], purified recombinant sCD13 is able to support monocytic cell adhesion, suggesting that CD13 functions as an adhesion molecule to directly mediate cell–cell interactions. However, our observation that sCD13 efficiently blocks the adhesion of anti-CD13-treated monocytic cells but has only a modest effect on mAb-treated HUVEC suggests differential binding as a result of alternately glycosylated CD13 forms or an indirect heterophilic CD13–CD13 interaction, possibly via an "adaptor/bridging" molecule on the monocytic cell that is activated by CD13 cross-linking and enables it to bind to CD13 on the monolayers. The carbohydrate-binding protein galectin-3 has been shown to regulate monocyte adhesion and transendothelial migration [51] and is also a CD13L ligand that participates in

CD13-induced monocytic cell adhesion [18]. In preliminary studies, CD13-mediated monocytic cell/endothelial interactions are partially blocked by anti-galectin-3 antibodies, consistent with a contributory role for galectin-3 in CD13-induced adhesion (data not shown). Thus, it is possible that as other adhesion molecules, CD13 establishes homophilic and heterophilic (galectin-3-mediated) interactions, which would explain the incomplete block with sCD13 or anti-galectin-3 antibodies. A homophilic interaction could be the result of CD13 clustering, inducing an increase in avidity, as has been proposed for integrins, cadherins, and other cellular adhesion molecules [52–54] and thus, may also participate in CD13-induced adhesion on endothelial cells. Alternatively, clustering could result in a conformational change, exposing cryptic epitopes (as has been reported for anti-CD13 antibodies of the same specificity as our active mAb [32]) that mediate adhesion. In this regard, under basal conditions, CD13 may exist in an "inactive" conformation, which clustering converts to an "active", oligomeric conformation now capable of interacting with inactive molecules on the untreated cells. CD13 ligation in both populations would produce only active forms incapable of establishing productive interactions and may explain the impaired inflammatory cell infiltration in vivo in the presence of antibodies (see below). The fact that sCD13 only blocks clustered CD13 suggests that it is in an inactive conformation (perhaps as a result of alternative glycosylation), which also explains its inability to induce adhesion.
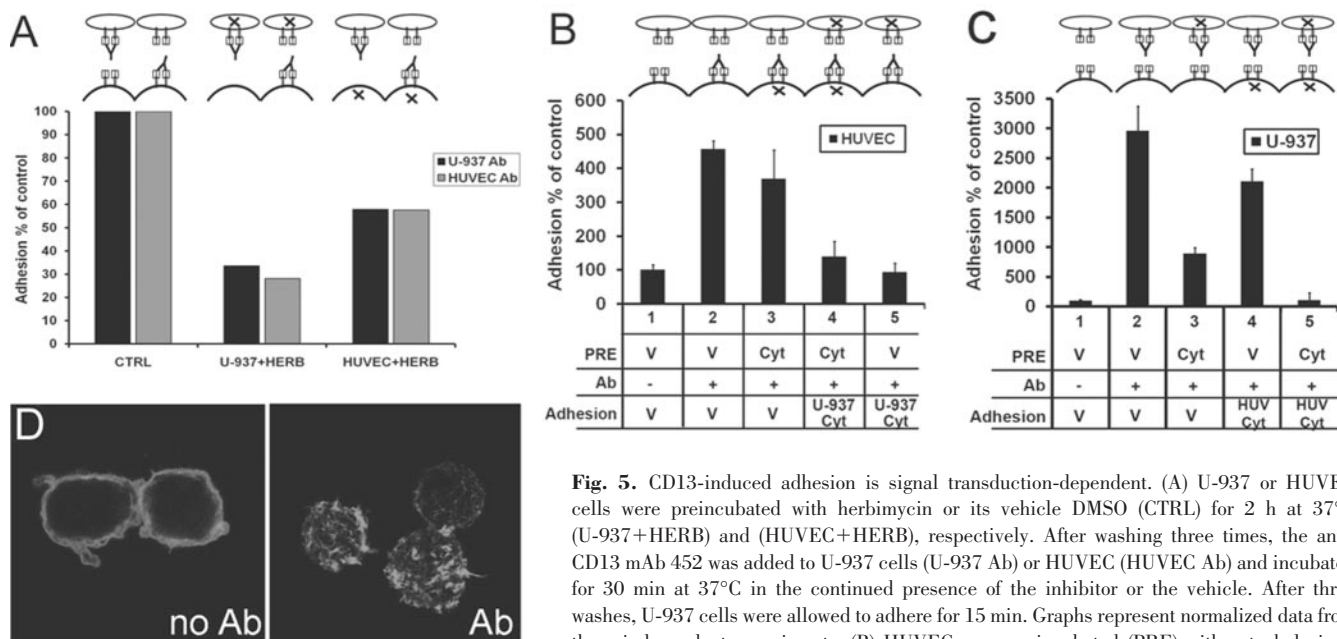
Fig. 5. CD13-induced adhesion is signal transduction-dependent. (A) U-937 or HUVEC cells were preincubated with herbimycin or its vehicle DMSO (CTRL) for 2 h at 37°C (U-937+HERB) and (HUVEC+HERB), respectively. After washing three times, the anti-CD13 mAb 452 was added to U-937 cells (U-937 Ab) or HUVEC (HUVEC Ab) and incubated for 30 min at 37°C in the continued presence of the inhibitor or the vehicle. After three washes, U-937 cells were allowed to adhere for 15 min. Graphs represent normalized data from three independent experiments. (B) HUVEC were preincubated (PRE) with cytochalasin-D 200 nM for 30 min at 37°C before addition of the anti-CD13 mAb (Ab), and adhesion was allowed to proceed in the presence of the same concentration of cytochalasin-D (Cyt) or an equivalent volume of vehicle (V). Two extra samples were included (Lanes 4 and 5), in which U-937 cells had been pretreated with cytochalasin-D 2 μM (U-937-Cyt) for 30 min at 37°C before the assay. The graph represents the arithmetic mean and SD of two independent experiments. (C) U-937 cells were preincubated with 2 μM cytochalasin-D or the vehicle. After 30 min at 37°C, the anti-CD13 mAb 452 was added (Ab) in the continued presence of the vehicle or cytochalasin. Finally, cells were washed five times and allowed to adhere to HUVEC for 15 min (Adhesion) in the presence of vehicle or cytochalasin-D at the same concentration. In Lanes 4 and 5, mAb-treated (1.0 μg/ml) U-937 cells preincubated with cytochalasin or vehicle were allowed to adhere onto cytochalasin-treated HUVEC (HUV Cyt). Adhesion was quantified as above. (D) Control U-937 cells (no Ab) or cells treated with the anti-CD13 mAb 452 for 15 min at 37°C (Ab) were fixed, permeabilized, stained with tetramethyl rhodamine isothiocyanate-conjugated phalloidin, and analyzed by confocal microscopy.

In addition to the architecture of the CD13 interaction, the downstream consequences of its ligation are an important issue. In monocytic cells, the principal result of CD13 clustering appears to be a signaling event involving tyrosine phosphorylation and Ca^{++} fluxing (Supplemental Fig. 4), as shown for other anti-CD13 mAb [16]. Extending these observations, we show that these processes result in requisite actin polymerization, as demonstrated by complete abrogation of CD13-induced adhesion by cytochalasin-D. Subsequently, CD13-induced actin polymerization leads to the formation of filopodial structures, as seen with cross-linking of other membrane receptors and other activating stimuli [43, 55]. These filopodial structures express high levels of adhesion molecules and membrane enzymes at their tips [56–58], underscoring the potential relevance of CD13-induced filopodia formation in monocyte adhesion. Pertinent to our study, some viruses use filopodia to increase the efficiency of infection and possibly for receptor interaction [59, 60]. As HCoV-229E cross-linking of CD13 increases monocytic cell adhesion, these may induce filopodia formation and thereby modulate physiologic processes to their advantage. Exploration of the consequences of active HCoV-229E infection on monocyte adhesion is underway.

The striking reduction in immune cell accumulation after treatment with anti-CD13 antibody in the in vivo model of peritonitis suggests a contributory role for CD13 in physiologic inflammatory processes, although the precise mechanism remains to be determined. Although we initially expected an increase in migration as a result of increased adhesion, our additional observations would also be consistent with de-creased transmigration in the presence of anti-CD13 mAb. As we have excluded cell death as a result of antibody-dependent mechanisms, the most straightforward explanation is that the continuous presence of circulating mAb blocks CD13 adhesion, presumably as a result of blocking binding sites or "hyperactivating" endothelial and monocytic CD13 to preclude binding, similar to our in vitro observations. Alternatively, although the effect of CD13 cross-linking on monocytic cell adhesion is apparent within 5 min of addition to the endothelial monolayer, our in vitro kinetic studies indicate that the adhesion diminishes to less than 50% of original values after 1 h of coculture, suggesting that the cells bind transiently and then detach, consistent with our observations in homotypic leukocyte adhesion [17]. It is possible that the signal induced by CD13 ligation is biphasic, first inducing adhesion via CD13–CD13 interactions and at later times, is antiadhesive, perhaps rendering cells refractory to subsequent adhesion via classical pathways. Another potential explanation is the CD13 ligation-dependent induction of HA, which if it occurs in vivo, could prevent monocyte/endothelial interactions and transmigration. However, we see no evidence of cellular aggregates in our examination of tissues from treated versus untreated animals, nor are cells aggregated in the adhesion assays at any time of our time-points. Finally, we cannot exclude the interaction of anti-CD13 antibodies with circulating sCD13, which may possibly affect transmigration by an undetermined mechanism. Experiments to distinguish among these possibilities are currently under way. Finally, the blocked infiltration of multiple cell types in this model implies that CD13 may regulate
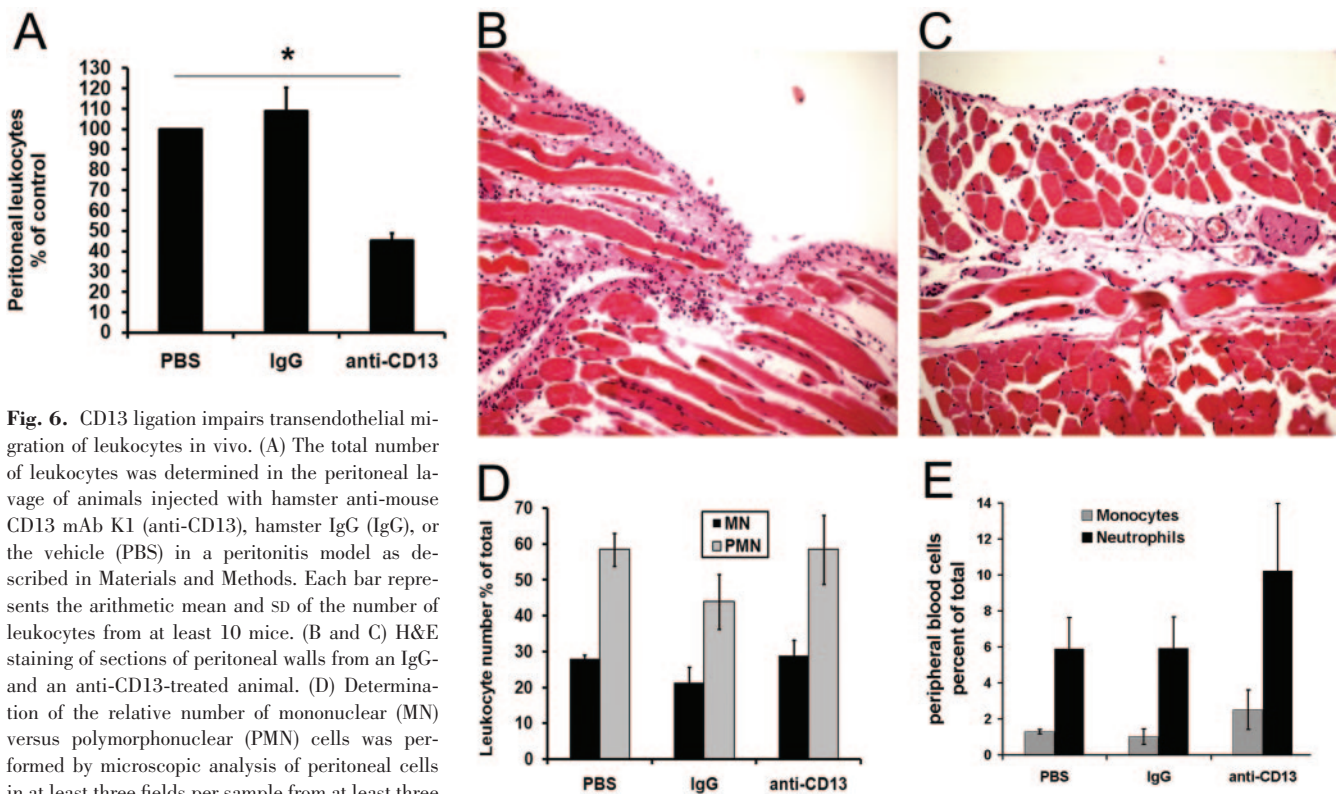
Fig. 6. CD13 ligation impairs transendothelial migration of leukocytes in vivo. (A) The total number of leukocytes was determined in the peritoneal lavage of animals injected with hamster anti-mouse CD13 mAb K1 (anti-CD13), hamster IgG (IgG), or the vehicle (PBS) in a peritonitis model as described in Materials and Methods. Each bar represents the arithmetic mean and SD of the number of leukocytes from at least 10 mice. (B and C) H&E staining of sections of peritoneal walls from an IgG- and an anti-CD13-treated animal. (D) Determination of the relative number of mononuclear (MN) versus polymorphonuclear (PMN) cells was performed by microscopic analysis of peritoneal cells in at least three fields per sample from at least three mice per group. (E) Determination of the relative number of monocytes (CD11b+/GR1−) versus polymorphonuclear (CD11b/Gr1 double-positive) cells in the circulation was performed by flow cytometric analysis of the peripheral blood from at least three mice per group. *, $P < 0.05$, unpaired Student's t-test.

migration of other immune cells such as neutrophils and activated T cells that also express significant amounts of CD13 [11].

The contribution of the enzymatic activity of CD13 is germane to its function in any capacity. We find that the most active antibodies are those that do not block enzymatic activity, suggesting that CD13 functions in an enzyme-independent manner. Additionally, we show that treatment with the CD13 inhibitor bestatin has no effect on mAb-induced adhesion nor does it induce adhesion itself. Alternatively, similar to mAb, binding and cleavage of peptide substrates to CD13 induce conformational changes that expose cryptic epitopes [32], suggesting that enzymatic cleavage of substrate may "prime" CD13 by exposing epitopes necessary for clustering. Indeed, in preliminary studies, treatment with peptide substrates significantly potentiates anti-CD13-induced adhesion (not shown), consistent with an increase in epitopes enhancing clustering and subsequent signaling. Further studies are necessary to determine the role of CD13 enzymatic activity and the mechanisms of CD13 activation in intercellular adhesion.

Finally, the issue of a putative CD13L is obviously critical to the relevance of the current study. Although it is premature to speculate as to its nature, strong support for the existence of an endogenous ligand comes from the numerous examples of viruses that co-opt cellular adhesion molecules as receptors and upon infection, cross-link their receptors and alter the adhesive properties of the infected cell, thereby exploiting a physiologic function to gain access to extravascular tissues [61–67]. Furthermore, the present study is relevant to diseases such as inflammatory bowel diseases associated with cytomegalovirus infection that produce high-titer circulating, anti-CD13 autoantibodies of the same epitope specificity as our activating clones [17], which could potentially play a role in these inflammatory processes [68, 69]. In addition, high concentrations of circulating sCD13 have been described in some inflammatory diseases [70, 71], raising the possibility that this acts as an endogenous modulator of CD13-mediated adhesion. Therefore, our identification of CD13 as an adhesion molecule mediating monocyte/endothelial interactions opens a novel area of research into the role of CD13 in inflammatory processes and disease.

ACKNOWLEDGMENTS

REFERENCES

1. Muller, W. A. (2001) Migration of leukocytes across endothelial junctions: some concepts and controversies. *Microcirculation* **8,** 181–193.
2. Luster, A. D., Alon, R., von Andrian, U. H. (2005) Immune cell migration in inflammation: present and future therapeutic targets. *Nat. Immunol.* **6,** 1182–1190.

3. Salmi, M., Jalkanen, S. (2005) Cell-surface enzymes in control of leukocyte trafficking. *Nat. Rev. Immunol.* **5,** 760–771.

4. Bunting, K. D., Bradley, H. L., Hawley, T. S., Moriggl, R., Sorrentino, B. P., Ihle, J. N. (2002) Reduced lymphomyeloid repopulating activity from adult bone marrow and fetal liver of mice lacking expression of STAT5. *Blood* **99,** 479–487.

5. Albiston, A. L., Ye, S., Chai, S. Y. (2004) Membrane bound members of the M1 family: more than aminopeptidases. *Protein Pept. Lett.* **11,** 491–500.

6. Look, A. T., Ashmun, R. A., Shapiro, L. H., Peiper, S. C. (1989) Human myeloid plasma membrane glycoprotein CD13 (gp150) is identical to aminopeptidase N. *J. Clin. Invest.* **83,** 1299–1306.

7. Pasqualini, R., Koivunen, E., Kain, R., Lahdenranta, J., Sakamoto, M., Stryhn, A., Ashmun, R. A., Shapiro, L. H., Arap, W., Ruoslahti, E. (2000) Aminopeptidase N is a receptor for tumor-homing peptides and a target for inhibiting angiogenesis. *Cancer Res.* **60,** 722–727.

8. Bhagwat, S. V., Lahdenranta, J., Giordano, R., Arap, W., Pasqualini, R., Shapiro, L. H. (2001) CD13/APN is activated by angiogenic signals and is essential for capillary tube formation. *Blood* **97,** 652–659.

9. Oh, P., Li, Y., Yu, J., Durr, E., Krasinska, K. M., Carver, L. A., Testa, J. E., Schnitzer, J. E. (2004) Subtractive proteomic mapping of the endothelial surface in lung and solid tumors for tissue-specific therapy. *Nature* **429,** 629–635.

10. Ward, P. E., Benter, I. F., Dick, L., Wilk, S. (1990) Metabolism of vasoactive peptides by plasma and purified renal aminopeptidase M. *Biochem. Pharmacol.* **40,** 1725–1732.

11. Riemann, D., Kehlen, A., Langner, J. (1999) CD13—not just a marker in leukemia typing. *Immunol. Today* **20,** 83–88.

12. Yeager, C. L., Ashmun, R. A., Williams, R. K., Cardellichio, C. B., Shapiro, L. H., Look, A. T., Holmes, K. V. (1992) Human aminopeptidase N is a receptor for human coronavirus 229E. *Nature* **357,** 420–422.

13. Mina-Osorio, P., Ortega, E. (2004) Signal regulators in FcR-mediated activation of leukocytes? *Trends Immunol.* **25,** 529–535.

14. Sjostrom, H., Noren, O., Olsen, J. (2000) Structure and function of aminopeptidase N. *Adv. Exp. Med. Biol.* **477,** 25–34.

15. Mina-Osorio, P., Ortega, E. (2005) Aminopeptidase N (CD13) functionally interacts with Fc{γ}Rs in human monocytes. *J. Leukoc. Biol.* **77,** 1008–1017.

16. Navarrete Santos, A., Langner, J., Riemann, D. (2000) Enzymatic activity is not a precondition for the intracellular calcium increase mediated by mAbs specific for aminopeptidase N/CD13. *Adv. Exp. Med. Biol.* **477,** 43–47.

17. Mina-Osorio, P., Shapiro, L. H., Ortega, E. (2006) CD13 in cell adhesion: aminopeptidase N (CD13) mediates homotypic aggregation of monocytic cells. *J. Leukoc. Biol.* **79,** 719–730.

18. Mina-Osorio, P., Soto-Cruz, I., Ortega, E. (2007) A role for galectin-3 in CD13-mediated homotypic aggregation of monocytes. *Biochem. Biophys. Res. Commun.* **353,** 605–610.

19. Obeso, J., Weber, J., Auerbach, R. (1990) A hemangioendothelioma-derived cell line: its use as a model for the study of endothelial cell biology. *Lab. Invest.* **63,** 259–269.

20. Breslin, J. J., Mork, I., Smith, M. K., Vogel, L. K., Hemmila, E. M., Bonavia, A., Talbot, P. J., Sjostrom, H., Noren, O., Holmes, K. V. (2003) Human coronavirus 229E: receptor binding domain and neutralization by soluble receptor at 37ºC. *J. Virol.* **77,** 4435–4438.

21. Chen, H., Kinzer, C. A., Paul, W. E. (1996) p161, a murine membrane protein expressed on mast cells and some macrophages, is mouse CD13/aminopeptidase N. *J. Immunol.* **157,** 2593–2600.

22. Sturman, L. S., Holmes, K. V., Behnke, J. (1980) Isolation of coronavirus envelope glycoproteins and interaction with the viral nucleocapsid. *J. Virol.* **33,** 449–462.

23. Melnicoff, M. J., Horan, P. K., Morahan, P. S. (1989) Kinetics of changes in peritoneal cell populations following acute inflammation. *Cell. Immunol.* **118,** 178–191.

24. Henderson, R. B., Hobbs, J. A., Mathies, M., Hogg, N. (2003) Rapid recruitment of inflammatory monocytes is independent of neutrophil migration. *Blood* **102,** 328–335.

25. Buehler, A., van Zandvoort, M. A. M. J., Stelt, B. J., Hackeng, T. M., Schrans-Stassen, B. H. G. J., Bennaghmouch, A., Hofstra, L., Cleutjens, J. P. M., Duijvestijn, A., Smeets, M. B., de Kleijn, D. P. V., Post, M. J., de Muinck, E. D. (2006) cNGR: a novel homing sequence for CD13/APN targeted molecular imaging of murine cardiac angiogenesis in vivo. *Arterioscler. Thromb. Vasc. Biol.* **26,** 2681–2687.

26. Kido, A., Krueger, S., Haeckel, C., Roessner, A. (1999) Possible contribution of aminopeptidase N (APN/CD13) to invasive potential enhanced by interleukin-6 and soluble interleukin-6 receptor in human osteosarcoma cell lines. *Clin. Exp. Metastasis* **17,** 857–863.

27. Takano, T., Hohdatsu, T., Toda, A., Tanabe, M., Koyama, H. (2007) TNF-α, produced by feline infectious peritonitis virus (FIPV)-infected macrophages, upregulates expression of type II FIPV receptor feline aminopeptidase N in feline macrophages. *Virology* **364,** 64–72.

28. Kehlen, A., Lendeckel, U., Dralle, H., Langner, J., Hoang-Vu, C. (2003) Biological significance of aminopeptidase N/CD13 in thyroid carcinomas. *Cancer Res.* **63,** 8500–8506.

29. Hatanaka, Y., Ashida, H., Hashizume, K., Fukuda, I., Sano, T., Yamaguchi, Y., Endo, T., Tani, Y., Suzukia, K., Danno, G., Tani, K., Ogushi, F., Shimizu, T., Sone, S., van der Velden, V. H., Naber, B. A., van Hal, P. T., Overbeek, S. E., Hoogsteden, H. C., Versnel, M. A. (2002) Up-regulation of CD13/aminopeptidase N induced by phorbol ester is involved in redox regulation and tumor necrosis factor α production in HL-60 cells. *Inflammation* **26,** 175–181.

30. Menrad, A., Speicher, D., Wacker, J., Herlyn, M. (1993) Biochemical and functional characterization of aminopeptidase N expressed by human melanoma cells. *Cancer Res.* **53,** 1450–1455.

31. Ashmun, R. A., Shapiro, L. H., Look, A. T. (1992) Deletion of the zinc-binding motif of CD13/aminopeptidase N molecules results in loss of epitopes that mediate binding of inhibitory antibodies. *Blood* **79,** 3344–3349.

32. Xu, Y., Wellner, D., Scheinberg, D. A. (1997) Cryptic and regulatory epitopes in CD13/aminopeptidase N. *Exp. Hematol.* **25,** 521–529.

33. Suda, H., Takita, T., Aoyagi, T., Umezawa, H. (1976) The structure of bestatin. *J. Antibiot. (Tokyo)* **29,** 100–101.

34. Barber, K. M., Pinero, A., Truskey, G. A. (1998) Effects of recirculating flow on U-937 cell adhesion to human umbilical vein endothelial cells. *Am. J. Physiol.* **275,** H591–H599.

35. Barry, O. P., Pratico, D., Savani, R. C., FitzGerald, G. A. (1998) Modulation of monocyte-endothelial cell interactions by platelet microparticles. *J. Clin. Invest.* **102,** 136–144.

36. Weber, C., Negrescu, E., Erl, W., Pietsch, A., Frankenberger, M., Ziegler-Heitbrock, H. W., Siess, W., Weber, P. C. (1995) Inhibitors of protein tyrosine kinase suppress TNF-stimulated induction of endothelial cell adhesion molecules. *J. Immunol.* **155,** 445–451.

37. van Wetering, S., van den Berk, N., van Buul, J. D., Mul, F. P., Lommerse, I., Mous, R., ten Klooster, J. P., Zwaginga, J. J., Hordijk, P. L. (2003) VCAM-1-mediated Rac signaling controls endothelial cell-cell contacts and leukocyte transmigration. *Am. J. Physiol. Cell Physiol.* **285,** C343–C352.

38. Delmas, B., Gelfi, J., L'Haridon, R., Vogel, L. K., Sjostrom, H., Noren, O., Laude, H. (1992) Aminopeptidase N is a major receptor for the enteropathogenic coronavirus TGEV. *Nature* **357,** 417–420.

39. Carman, C. V., Jun, C. D., Salas, A., Springer, T. A. (2003) Endothelial cells proactively form microvilli-like membrane projections upon intercellular adhesion molecule 1 engagement of leukocyte LFA-1. *J. Immunol.* **171,** 6135–6144.

40. Barreiro, O., Yanez-Mo, M., Serrador, J. M., Montoya, M. C., Vicente-Manzanares, M., Tejedor, R., Furthmayr, H., Sanchez-Madrid, F. (2002) Dynamic interaction of VCAM-1 and ICAM-1 with moesin and ezrin in a novel endothelial docking structure for adherent leukocytes. *J. Cell Biol.* **157,** 1233–1245.

41. Curnis, F., Arrigoni, G., Sacchi, A., Fischetti, L., Arap, W., Pasqualini, R., Corti, A. (2002) Differential binding of drugs containing the NGR motif to CD13 isoforms in tumor vessels, epithelia, and myeloid cells. *Cancer Res.* **62,** 867–874.

42. Watson, J. M., Harding, T. W., Golubovskaya, V., Morris, J. S., Hunter, D., Li, X., Haskill, J. S., Earp, H. S. (2001) Inhibition of the calcium-dependent tyrosine kinase (CADTK) blocks monocyte spreading and motility. *J. Biol. Chem.* **276,** 3536–3542.

43. Vicente-Manzanares, M., Sanchez-Madrid, F. (2004) Role of the cytoskeleton during leukocyte responses. *Nat. Rev. Immunol.* **4,** 110–122.

44. Carman, C. V., Springer, T. A. (2003) Integrin avidity regulation: are changes in affinity and conformation underemphasized? *Curr. Opin. Cell Biol.* **15,** 547–556.

45. Santos, A. N., Langner, J., Herrmann, M., Riemann, D. (2000) Aminopeptidase N/CD13 is directly linked to signal transduction pathways in monocytes. *Cell. Immunol.* **201,** 22–32.

46. Schenkel, A. R., Mamdouh, Z., Muller, W. A. (2004) Locomotion of monocytes on endothelium is a critical step during extravasation. *Nat. Immunol.* **5,** 393–400.

47. Imhof, B. A., Aurrand-Lions, M. (2004) Adhesion mechanisms regulating the migration of monocytes. *Nat. Rev. Immunol.* **4,** 432–444.

48. Pyszniak, A. M., Welder, C. A., Takei, F. (1994) Cell surface distribution of high-avidity LFA-1 detected by soluble ICAM-1-coated microspheres. *J. Immunol.* **152,** 5241–5249.

49. Lobb, R. R., Chi-Rosso, G., Leone, D. R., Rosa, M. D., Bixler, S., Newman, B. M., Luhowskyj, S., Benjamin, C. D., Dougas, I. G., Goelz, S. E., et al. (1991) Expression and functional characterization of a soluble form of endothelial-leukocyte adhesion molecule 1. *J. Immunol.* **147,** 124–129.

50. Meyer, D. M., Dustin, M. L., Carron, C. P. (1995) Characterization of intercellular adhesion molecule-1 ectodomain (sICAM-1) as an inhibitor of lymphocyte function-associated molecule-1 interaction with ICAM-1. *J. Immunol.* **155,** 3578–3584.

51. Hsu, D. K., Yang, R. Y., Pan, Z., Yu, L., Salomon, D. R., Fung-Leung, W. P., Liu, F. T. (2000) Targeted disruption of the galectin-3 gene results in attenuated peritoneal inflammatory responses. *Am. J. Pathol.* **156,** 1073–1083.

52. Tsuiji, H., Xu, L., Schwartz, K., Gumbiner, B. M. (2007) Cadherin conformations associated with dimerization and adhesion. *J. Biol. Chem.* **282,** 12871–12882.

53. Yap, A. S., Brieher, W. M., Pruschy, M., Gumbiner, B. M. (1997) Lateral clustering of the adhesive ectodomain: a fundamental determinant of cadherin function. *Curr. Biol.* **7,** 308–315.

54. Miller, J., Knorr, R., Ferrone, M., Houdei, R., Carron, C. P., Dustin, M. L. (1995) Intercellular adhesion molecule-1 dimerization and its consequences for adhesion mediated by lymphocyte function associated-1. *J. Exp. Med.* **182,** 1231–1241.

55. Salazar-Fontana, L. I., Barr, V., Samelson, L. E., Bierer, B. E. (2003) CD28 engagement promotes actin polymerization through the activation of the small Rho GTPase Cdc42 in human T cells. *J. Immunol.* **171,** 2225–2232.

56. Moore, K. L., Patel, K. D., Bruehl, R. E., Li, F., Johnson, D. A., Lichenstein, H. S., Cummings, R. D., Bainton, D. F., McEver, R. P. (1995) P-selectin glycoprotein ligand-1 mediates rolling of human neutrophils on P-selectin. *J. Cell Biol.* **128,** 661–671.

57. Erlandsen, S. L., Hasslen, S. R., Nelson, R. D. (1993) Detection and spatial distribution of the β 2 integrin (Mac-1) and L-selectin (LECAM-1) adherence receptors on human neutrophils by high-resolution field emission SEM. *J. Histochem. Cytochem.* **41,** 327–333.

58. Harris, J., Schwinn, N., Mahoney, J. A., Lin, H. H., Shaw, M., Howard, C. J., da Silva, R. P., Gordon, S. (2006) A vitellogenic-like carboxypeptidase expressed by human macrophages is localized in endoplasmic reticulum and membrane ruffles. *Int. J. Exp. Pathol.* **87,** 29–39.

59. Lehmann, M. J., Sherer, N. M., Marks, C. B., Pypaert, M., Mothes, W. (2005) Actin- and myosin-driven movement of viruses along filopodia precedes their entry into cells. *J. Cell Biol.* **170,** 317–325.

60. Sherer, N. M., Lehmann, M. J., Jimenez-Soto, L. F., Horensavitz, C., Pypaert, M., Mothes, W. (2007) Retroviruses can establish filopodial bridges for efficient cell-to-cell transmission. *Nat. Cell Biol.* **9,** 310–315.

61. Sasseville, V. G., Newman, W., Brodie, S. J., Hesterberg, P., Pauley, D., Ringler, D. J. (1994) Monocyte adhesion to endothelium in simian immunodeficiency virus-induced AIDS encephalitis is mediated by vascular cell adhesion molecule-1/α 4 β 1 integrin interactions. *Am. J. Pathol.* **144,** 27–40.

62. Hartshorn, K. L., White, M. R. (1999) Influenza A virus up-regulates neutrophil adhesion molecules and adhesion to biological surfaces. *J. Leukoc. Biol.* **65,** 614–622.

63. Kim, S. J., Nair, A. M., Fernandez, S., Mathes, L., Lairmore, M. D. (2006) Enhancement of LFA-1-mediated T cell adhesion by human T lymphotropic virus type 1 p12I1. *J. Immunol.* **176,** 5463–5470.

64. Mehl, A. M., Floettmann, J. E., Jones, M., Brennan, P., Rowe, M. (2001) Characterization of intercellular adhesion molecule-1 regulation by Epstein-Barr virus-encoded latent membrane protein-1 identifies pathways that cooperate with nuclear factor κ B to activate transcription. *J. Biol. Chem.* **276,** 984–992.

65. Stark, J. M., Godding, V., Sedgwick, J. B., Busse, W. W. (1996) Respiratory syncytial virus infection enhances neutrophil and eosinophil adhesion to cultured respiratory epithelial cells. Roles of CD18 and intercellular adhesion molecule-1. *J. Immunol.* **156,** 4774–4782.

66. Marker, O., Scheynius, A., Christensen, J. P., Thomsen, A. R. (1995) Virus-activated T cells regulate expression of adhesion molecules on endothelial cells in sites of infection. *J. Neuroimmunol.* **62,** 35–42.

67. Andersson, E. C., Christensen, J. P., Marker, O., Thomsen, A. R. (1994) Changes in cell adhesion molecule expression on T cells associated with systemic virus infection. *J. Immunol.* **152,** 1237–1245.

68. Rahbar, A., Bostrom, L., Soderberg-Naucler, C. (2006) Detection of cytotoxic CD13-specific autoantibodies in sera from patients with ulcerative colitis and Crohn's disease. *J. Autoimmun.* **26,** 155–164.

69. Soderberg, C., Sumitran-Karuppan, S., Ljungman, P., Moller, E. (1996) CD13-specific autoimmunity in cytomegalovirus-infected immunocompromised patients. *Transplantation* **61,** 594–600.

70. van Hensbergen, Y., Broxterman, H. J., Hanemaaijer, R., Jorna, A. S., van Lent, N. A., Verheul, H. M. W., Pinedo, H. M., Hoekman, K. (2002) Soluble aminopeptidase N/CD13 in malignant and nonmalignant effusions and intratumoral fluid. *Clin. Cancer Res.* **8,** 3747–3754.

71. Favaloro, E. J., Browning, T., Nandurkar, H. (1993) The hepatobiliary disease marker serum alanine aminopeptidase predominantly comprises an isoform of the hematological myeloid differentiation antigen and leukemia marker CD-13/gp150. *Clin. Chim. Acta* **220,** 81–90.